

Molecular Cobalt Catalysts Grafted onto Polymers for Efficient Hydrogen Generation Cathodes

Cheng-Bo Li,* Yilong Chu, Pengfei Xie, Lunqiao Xiong, Ning Wang, Hongyan Wang, and Junwang Tang*

A conjugated microporous polymer is in situ electropolymerized to form a basis for immobilization of a molecular catalyst onto glassy carbon. A cost-effective molecular catalyst is then grafted onto the polymer by π - π interactions as evidenced by X-ray photoelectron spectroscopy (XPS), Fourier transform infrared spectroscopy (FTIR), and UV-vis spectra. The prepared cathode represents a high activity toward hydrogen evolution (109 100 turnovers in 2 h) in mild acidic aqueous solutions with a $\approx 100\%$ faradaic efficiency. The cathode also shows a very good stability. In total, this article introduces a facile means to design and prepare a hydrogen generation cathode using widely available and inexpensive materials.

1. Introduction

It is anticipated that hydrogen will play a central role in the next several decades as climate change threatens the well-being of the planet.^[1] In this scenario, the development of advanced materials and techniques for electro- and photoelectrocatalytic hydrogen production has received increasing global attention.^[2] Molecular catalysts are attractive because the ligand environment allows for tuning of their reduction potentials and chemical

properties. To this end, the immobilization of soft molecular catalysts on hard electrodes is gaining interest.^[3] Although some versatile strategies have been reported for their immobilization onto metal oxide,^[4] carbon-based,^[5] and conductive electrode^[6] surfaces for applications in electro- and photoelectrocatalytic H₂ production, many systems are confined for implementation at scale due to being designed with synthetically challenging, including costly ligand manifolds (providing good stability and catalytic properties for catalysts), difficult linker design (considering their length, polarity, flexibility, conductivity, etc.), and necessary anchor components. An ideal

system would require minimal synthetic effort, only inexpensive materials, and have the capability to be directly tied to a renewable energy source to produce clean H₂ without further modification.^[7] Although immobilization via drop-casting methods and other electrostatic-based deposition techniques used to affix molecules to surfaces offer ease of assembly, the development of more precise surface attachment chemistries could offer additional control over orientation of attached components, surface loading, passivation of the substrate, and interfacial energetics.^[8]


In this article, we report polythiophene analogue (PTTB), polymerized by 1,3,5-tri(thiophen-2-yl)benzene (TTB), as one kind of conjugated microporous polymer networks which could serve as a surface-grafted organic coating for assembly of hydrogen-evolving molecular catalysts onto a glassy carbon (GC) electrode or fluorine doped tin oxide (FTO) glass electrode (**Scheme 1**). Many thiophene-based conjugated microporous polymer networks have been reported with excellent electrical, electrochemical, and optical properties, are usually cheap, and can be conveniently prepared at large scale via chemical or electrochemical approaches, thus our approach provides an incredibly versatile option open to nearly all aromatic systems.^[9] Their enlarged surface area and rich π -bonds also provide facile platforms for immobilization π -bond-rich molecular catalysts by π - π stacking and hydrophobic interactions. Meanwhile, the complicated design of linkers and anchors for molecule immobilization could be avoided. Especially, non-water-soluble molecular catalysts on the fabricated electrodes would be more stable due to the lack of competition dissolution into water.

Recently, we and Du's group reported a series of metal-salen complexes as hydrogen-evolving catalysts for homogeneous photo- and electrocatalytic hydrogen evolution.^[10] These metal-salen complexes have merits of accessibility, cost-effective

Dr. C.-B. Li, Y. Chu, P. Xie, Dr. N. Wang
Key Laboratory of Synthetic and Natural Functional Molecule of the
Ministry of Education
The Energy and Catalysis Hub
College of Chemistry & Materials Science
Northwest University
Xi'an 710127, P. R. China
E-mail: lcb123@nwu.edu.cn

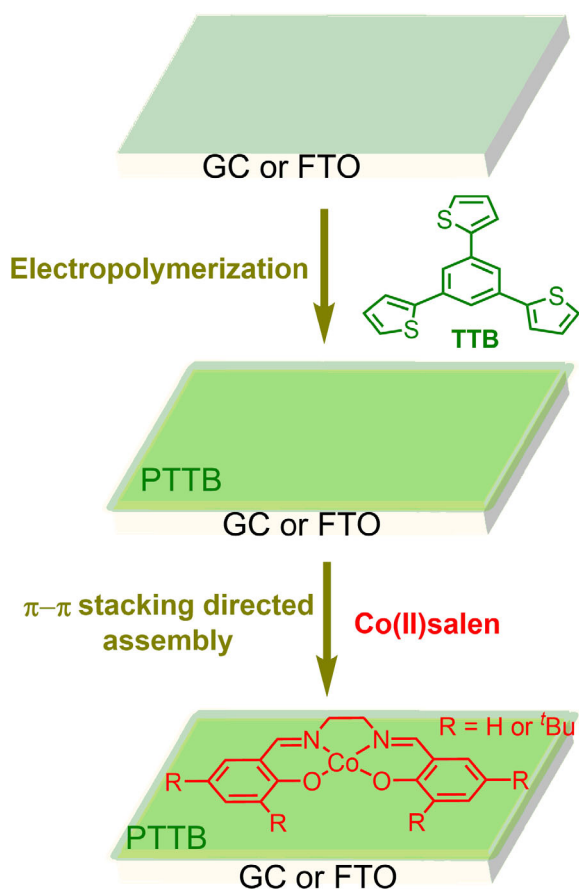
L. Xiong, Prof. J. Tang
Department of Chemical Engineering
UCL
Torrington Place, London WC1E 7JE, UK
E-mail: Junwang.tang@ucl.ac.uk

Dr. H. Wang
School of Chemistry and Chemical Engineering
Shaanxi Normal University
Xi'an 710119, P. R. China

 The ORCID identification number(s) for the author(s) of this article can be found under <https://doi.org/10.1002/solr.202000281>.

© 2020 The Authors. Published by Wiley-VCH GmbH. This is an open access article under the terms of the Creative Commons Attribution License, which permits use, distribution and reproduction in any medium, provided the original work is properly cited.

DOI: 10.1002/solr.202000281



Scheme 1. Schematic representation of the fabrication method used to assemble modified cathodes.

synthesis, and hydrogen-evolving performance.^[11] In addition, they are electroneutral, water insoluble, and rich in π -bonds, exhibiting very good compatibility with conjugated polymers to construct composite catalyst in the current work. Therefore, this work represents a facile method toward developing an integrated cathode for electrocatalytic hydrogen evolution on molecular catalysts immobilized onto GC or FTO substrates, in which PTTB is an excellent linker for cobalt(II)-salen complex. Furthermore, using a conjugated microporous polymer for surface functionalization allows use of a broad range of π -bonds, giving additional control over surface loading capacity and attachment stability of catalysts as new materials and discoveries.

2. Results and Discussions

Fabrication of cobalt(II)-salen complex immobilized electrodes via a polymeric interface starts with electropolymerization of TTB monomers to form conjugated microporous polymer PTTB on FTO or GC by cyclic voltammetry (CV) method. This approach provides polymers as a thin film bearing rich π -bonds binding sites and significantly increases the geometric area loading capacity of catalysts on the electrode. After the polymerization, wet chemical treatment of the polymer-modified surface using a solution of cobalt(II)-salen complex is conducted

followed by thoroughly rinsed with corresponding solvents (Scheme 1). Fourier transform infrared spectroscopy (FTIR), X-ray photoelectron spectroscopy (XPS), and transmission electron microscopy (TEM) provide consistent evidence that the molecular catalyst attaches onto the polymer surface.

2.1. Electrodeposition and Characterization of PTTB

The TTB monomers were initially polymerized by multicycled CV in anhydrous dichloromethane as the reported conditions.^[9b] Open-top polymer tubes and cauliflower-like polymer pellets could be obtained under different CV cycles (Figure S1, Supporting Information). However, the deposited PTTB film fractured and stripped easily after separating from the electrolyte due to the quick evaporation of dichloromethane. In another way, the PTTB polymer could be deposited in the acetonitrile, having good integrity and adhesion on the electrode. To uniform the polymer samples, the CV electropolymerization process in acetonitrile was conducted for ten cycles (Figure 1a).

The morphological characteristics of PTTB were then characterized using scanning electron microscopy (SEM) and TEM. Figure 1b shows a top-view SEM image of the PTTB, showing the morphology as a thin film. The thickness of the film was characterized by obtaining cross-sectional SEM images of approximately 223 nm (Figure 1c). The detailed morphology of the PTTB was characterized by TEM analysis (Figure S2, Supporting Information); PTTB exhibits a 2D agglomerated layered lamellar-like morphology. In addition, a lattice spacing of 0.63 nm and interplanar distance of 0.64 nm were observed in the high-resolution TEM image. The polycrystalline nature of PTTB was also confirmed by selected area electron diffraction (SAED) patterns (Figure S2b, Supporting Information).

FTIR spectra exhibited the vibration change from monomer TTB to PTTB (Figure 1d). The frequencies of the four absorption bands centered in the 2800–3000 cm^{-1} range and the broadening of the absorption peaks in the 900–1800 cm^{-1} range show the vibration of the C–H groups and C=C groups of backbone change after polymerization. UV-vis spectra of PTTB deposited on FTO were further detected. The background signal of FTO was deducted. Two absorption regions around 340–450 nm and 500–700 nm were observed, which shifted to the red direction as CV cycles increased (Figure S3, Supporting Information).

2.2. Assembly of Cobalt-Salen to PTTB

Cobalt-salen complexes can be physisorbed on PTTB deposited on an electrode substrate through the establishment of π - π stacking interactions between the π -rich backbone salen ligands and PTTB motifs. FTIR characterization shows the formation of PTTB-cobalt(II)-salen (PTTB-Cosalen), which could be verified from the appearance of the absorption peaks in the 3040–3130 cm^{-1} range and 1360–1485 cm^{-1} range (Figure 2a). These vibration signals are only existing in cobalt(II)-salen and could be ascribed to the vibration of the C–H groups and C=N groups.

The presence of intact Co complex is further confirmed by XPS (Figure 2b). Survey spectra of cobalt(II)-salen-modified PTTB show the presence of C, N, O, S, and Co elements of the

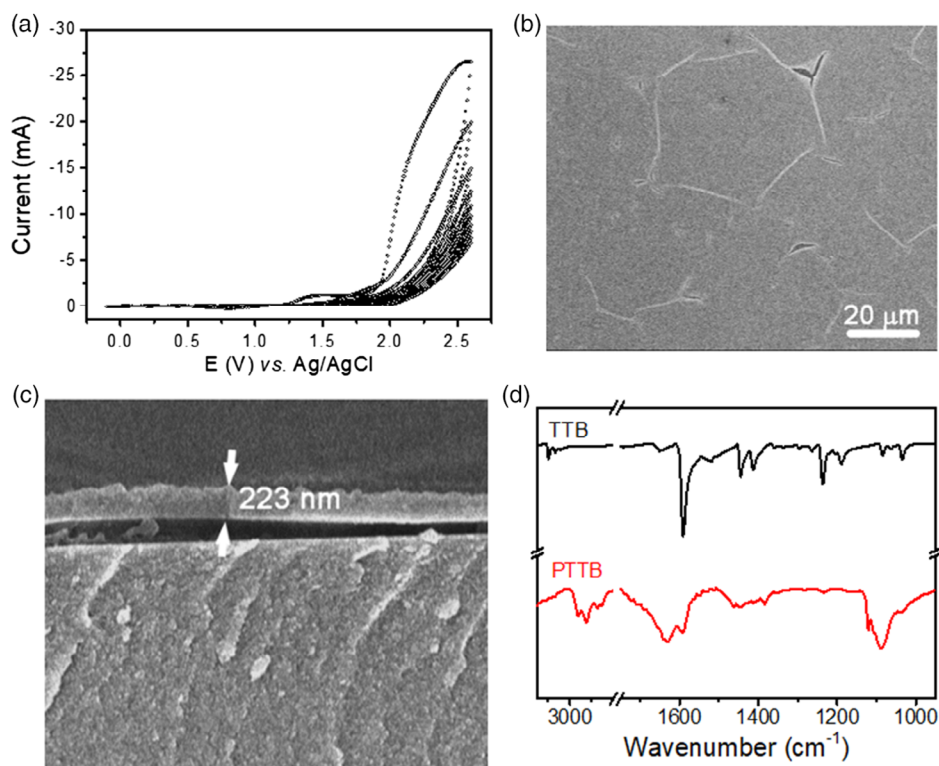


Figure 1. a) Cyclic voltammograms (ten scans at 200 mV s^{-1}) of the monomer TTB in $0.1 \text{ M Bu}_4\text{NClO}_4/\text{MeCN}$. b) SEM image of PTTB electrodeposited by CV. c) SEM cross-sectional image of a GC/PTTB electrode. d) FTIR transmission spectra of TTB (black), PTTB before (red).

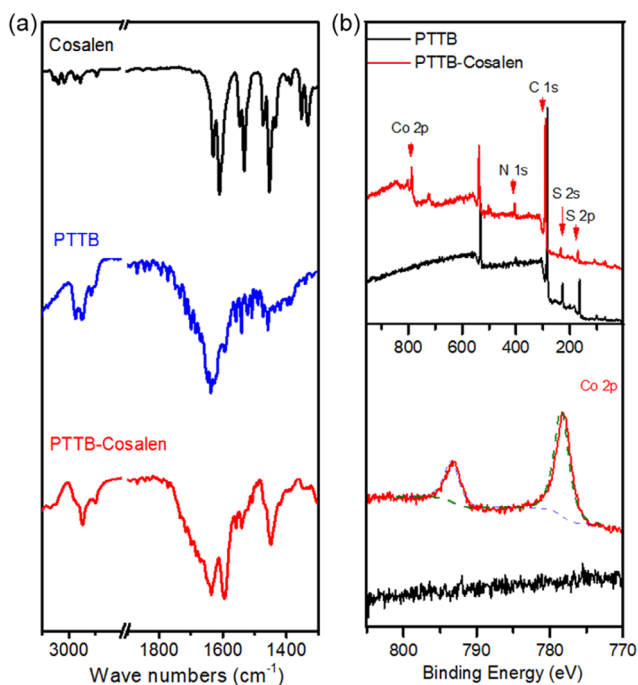


Figure 2. a) FTIR transmission spectra of Cosalen in KBr (black), PTTB in KBr (blue), and PTTB-Cosalen in KBr (red). b) Survey (up) and Co 2p core-level (down) spectra of pristine PTTB (black) and PTTB-Cosalen (red) supported on GC substrates.

catalyst and PTTB. N 1s core-level spectra of PTTB-Cosalen show a single feature centered at 398.4 eV which should be attributed to the salen ligand. In addition, Co 2p core-level spectra of PTTB-Cosalen show peaks centered at 778.3 eV ($2p_{3/2}$) and 793.5 eV ($2p_{1/2}$) with the expected 2:1 branching ratio, which are assigned to Co^{II} .^[12] Another peak with binding energies of $\approx 164.0 \text{ eV}$ are observed for PTTB-Cosalen, which corresponds to S 2p. The broad peaks at 168.0 eV is assigned to the shakeup satellites.^[6e] The full XPS spectra of PTTB-Cosalen samples are shown in Figure S4, Supporting Information. Based on the inductively coupled plasma mass spectrometry (ICP-MS) results of the acidic-digested sample of PTTB-Cosalen, the Co content was calculated to be $1.75 \times 10^{-9} \text{ mol}_{\text{Co}} \text{ cm}^{-2}$.

The aforementioned data support the assembly of PTTB with cobalt(II)-salen moieties assembled by π - π stacking. It is predictable a planner structure of the cobalt(II)-salen benefits the intimate contact with the PTTB film by π - π stacking interaction. Furthermore, we investigated four-tertiary-butyl-derived salen complex (cobalt(II)-^tBu-salen) to backward this viewpoint. The XPS analysis (Figure S5, Supporting Information) of PTTB-cobalt(II)-^tBu-salen (PTTB-Co(^tBu-salen)) shows a much lower Co:S (1:72) than that in PTTB-Cosalen (1:9).

2.3. Electrochemistry Studies

The electrochemistry of GC/PTTB-Cosalen was investigated by CV. Maximum average surface catalyst concentrations of $1.69 \times 10^{-10} \text{ mol}_{\text{Co}} \text{ cm}^{-2}$ are estimated from the integration of

the electrochemical wave (Figure S6, Supporting Information). This value is approximately 1/10 of that obtained from ICP-MS measurements of the sonicated and digested PTTB-Cosalen, suggesting that the majority of the cobalt centers are electrochemically inactive. The hydrophobic property of PTTB may impede the reaction of deep-seated Cosalen with water.

The new molecular-based GC/PTTB-Cosalen material is catalytically competent for H₂ evolution from fully aqueous electrolytes at a mild pH. A CV experiment recorded on a GC/PTTB-Cosalen electrode (Figure 3a, red solid line) was first conducted in acetate buffer solution (0.1 M, pH 4.5). A strong wave with a cathodic onset potential of $E_{\text{onset}} = -0.45$ V versus reversible hydrogen electrode (RHE) is observed as a result of catalytic reduction of protons to H₂. Testing of the same GC/PTTB electrode in identical conditions prior to catalyst adsorption showed minimal background current (Figure 3a, black solid line), confirming this activity as being directly a result of the catalyst's presence. We also tested the linear sweep voltammetry experiment recorded on a GC/PTTB-Co(^tBu-salen) electrode, a much weaker cathodic wave was observed (Figure 3a, blue solid line), indicating the branched molecular catalyst is not suitable for the GC/PTTB substrate due to the limited π - π interaction. Indeed, several other well-known catalysts such as μ -(1,3-propanedithiolato)-hexacarbonyldiiron (pdt-Fe₂S₂),^[13] cobalt diimine-dioxime complex (Co(DO)(DOH)pnBr₂),^[14] and cobalt tetraphenylporphyrin (CoTPP)^[15] were also assembled to form a GC/PTTB-catalyst electrode, albeit with much poorer catalytic performance (Figure S7, Supporting Information) due to either low amount loaded or hard to load. The loading amounts of Cosalen effect related different assembly time are

shown in Figure S8, Supporting Information, in which the 10 h assembly sample shows the highest catalytic current likely due to the highest amount of Cosalen loaded. Furthermore, O₂ tolerance of GC/PTTB-Cosalen was investigated in acetate buffer (pH 4.5, 0.1 M) by linear sweep voltammetry (LSV) scanning with air bubbling or N₂ protection (Figure 3b). Results revealed that O₂ had very limited impact on effectiveness of proton reduction by the grafted molecular catalyst which still displays good activity for H₂ evolution in the presence of O₂, indicating an excellent selectivity to proton reduction against O₂ reduction.

As the pH of the aqueous solution is lowered, an increase in current is observed (Figure S9, Supporting Information). A potential value of -0.63 V versus RHE was required to reach a current density of 1 mA cm^{-2} at pH 4.5. Tafel analysis (Figure S10, Supporting Information) gave a Tafel slope of 193 mV per decade and an exchange current density of $10^{-6.3} \text{ A cm}^{-2}$ geometric. This value is comparable with that reported for MWCNT/[Co(DO)(DOH)pnBr₂] ($10^{-6.5} \text{ A cm}^{-2}$ geometric)^[5a] and electropolymerized of Co(II) dibenzotetraaza annulene (CoTAA, $10^{-8} \text{ A cm}^{-2}$ geometric).^[16]

Controlled potential electrolysis (CPE) of GC/PTTB-Cosalen in acetate buffer solution (0.1 M, pH 4.5), measured at -0.75 V versus RHE, consumed 7.13 coulombs of charge after 2 h (Figure 3c,d). Although a broad current density was observed due to the bubbles generated on the electrode surface and their desorption matter, the current density stabilized after 2 h at a constant value of approximately 1 mA cm^{-2} . Analysis of the gas mixture in the headspace (Figure S11, Supporting Information) of the working compartment of the electrolysis cell by gas chromatography confirmed production of H₂ with a

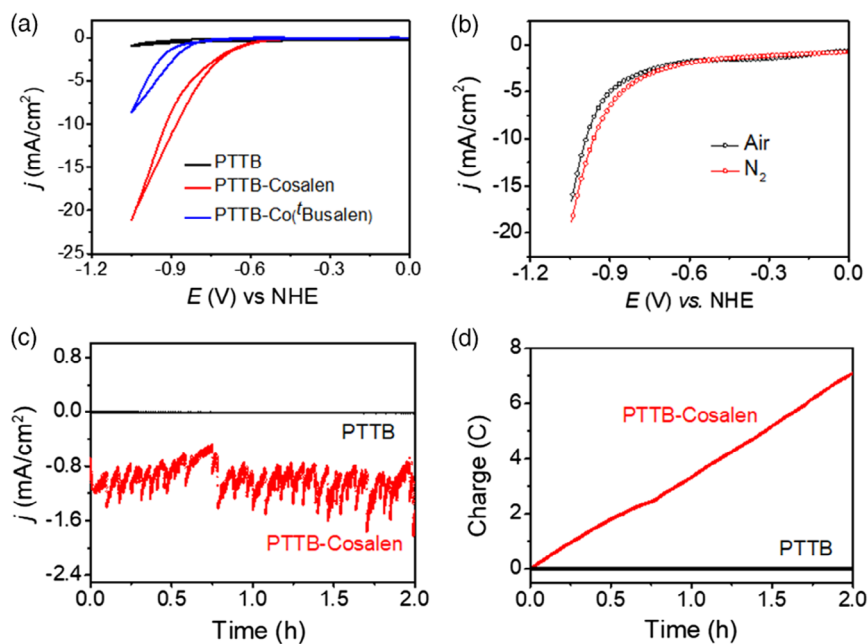


Figure 3. a) CV measurements recorded on a GC/PTTB-Cosalen electrode (red line) compared with that of GC/PTTB-Co(^tBu-salen) (blue line) and an unfunctionalized GC/PTTB electrode (black line) in acetate buffer (0.1 M, pH 4.5) at 100 mV s^{-1} . b) Oxygen resistance investigation run on a GC/PTTB-Cosalen in acetate buffer (0.1 M, pH 4.5). c) Evolution of the current density during an electrolysis experiment run on a GC/PTTB-Cosalen electrode (red dotted line) compared with that of a blank GC/PTTB electrode (black dotted line) at -0.75 V versus RHE in acetate buffer (0.1 M, pH 4.5). d) Charge passed during the same experiment for electrocatalytic H₂ production.

Table 1. Electrocatalytic proton reduction in aqueous solution using electrodes modified with molecular catalysts.

Electrode	TON	TOF [h^{-1}]	Ref.
PTTB-Cosalen	1.1×10^5	5.5×10^4	–
CNT/Ni($\text{P}_{\text{ph}}^2, \text{N}_{\text{C}_{12}\text{pyrene}}^2$) ₂	8.5×10^4	1.4×10^4	[9]
CNT/pPyCo	420	42	[10]
CNT/Ni($\text{P}_{\text{ph}}^2, \text{N}_{\text{CH}_2}^2$) ₂	1×10^5	1×10^4	[12]
RGO/Co($\text{S}_2\text{C}_6\text{H}_2\text{Cl}_2$) ₂	9.1×10^6	1.1×10^6	[13]
GC/CoTPP	26	17	[15]

Faradaic yield of approximately 100%. Considering that two electrons are required for the formation of a H_2 molecule and using the loading concentration of the catalyst ($1.75 \times 10^{-9} \text{ mol cm}^{-2}$) and the active surface concentration of the catalyst ($1.69 \times 10^{-10} \text{ mol cm}^{-2}$), we calculated a turnover number (TON) of 10 540 and 109 100, respectively. A turnover frequency (TOF) per grafted Co catalyst of 1.5 and 15.2 s^{-1} was calculated. The bulk electrolysis was then conducted under -0.6 V versus RHE. After 20 h electrolysis, the current density still retained 60% of the initial, indicating a very robust cathode (Figure S12, Supporting Information). Although the stability is not comparable with those reported in inorganic materials,^[17] its activity is superior to most of other obtained molecular catalyst-grafted electrodes (Table 1).^[5c,d,f,g,6b,18]

XPS analyses of GC/PTTB-Cosalen after electrochemical studies display peaks similar to the ones observed before electrolysis, suggesting that the material left on GC is stable under reductive and acidic conditions (Figure S13, Supporting Information). In the Co region, the two broad sets of signals that correspond to the $2\text{p}_{3/2}$ and $2\text{p}_{1/2}$ core levels are still observed. The absence of any peak below 780.9 eV excludes the presence of cobalt oxide or metallic cobalt on the surface. This observation clearly excludes any reductive transformation of the grafted molecular complex into the nanoparticle H_2 -CoCat material as reported molecular complexes in solution.^[19] The ICP-MS analysis of PTTB-Cosalen sample after 2 h electrolysis (-0.75 V vs RHE) showed that about 44% Cosalen still retained on the electrode (Table S1, Supporting Information).

3. Conclusions

We demonstrate here, for the first time, a cobalt-salen catalyst was grafted onto electropolymerized conjugated microporous polymer PTTB, which generated a very active electrocatalytic cathode for H_2 production from mildly acidic aqueous solutions. The electrode was cost-effective, efficient, and robust with a good stability. Around 109 100 turnovers were obtained during 2 h of electrolysis in an acetate buffer at a potential of -0.75 V versus RHE. The high catalytic activity also remained under O_2 exposure, proving an excellent selectivity to proton reduction. With the wide range of conjugated microporous polymer substrates and π -rich molecular catalysts available for deposition, a variety of materials for heterogeneous dihydrogen-generation catalysis could be developed, giving substantial possibility for materials

engineering. Applications in photoelectrocatalytic systems are of particular interest, and corresponding studies are underway.

4. Experimental Section

Materials: 1,3,5-Tri-(thiophen-2-yl)benzene (TTB), salicylaldehyde, anhydrous dichloromethane, acetonitrile, ethanediamine, and $\text{Co}(\text{Ac})_2 \cdot 6\text{H}_2\text{O}$ were purchased from Adamas Company (Shanghai, China). Tetrabutylammonium perchlorate (Bu_4NClO_4) was obtained from Aladdin (Shanghai, China). HAc buffer solutions were prepared by mixing 0.1 M HAc and 0.1 M NaAc. Cosalen complexes were prepared as previously reported methods.^[10a,b,d] All reagents were used without further purification.

Electropolymerization: All of the electropolymerization experiments were performed on a CHI600E electrochemical workstation (Chenhua, Shanghai, China) using a three-electrode system. Dichloromethane or acetonitrile solution (5 mL) containing 5 mM monomers and 0.1 M Bu_4NClO_4 was added to a glass electrochemical cell. Glassy carbon rods (diameter 3 mm), glassy carbon sheet ($1 \times 2 \text{ cm}^2$), SEM electrode (glassy carbon, diameter 3 mm), and FTO ($1 \times 2 \text{ cm}^2$, square resistance 5–7 Ω) were used as working electrodes, in combination with a platinum counter electrode and an Ag/Ag^+ electrode as the reference electrode. Electro polymerization was performed by CV method was performed from -0.7 to 2.0 V at a scan rate of 200 mV s^{-1} with different scan numbers.

Electrode Fabrication: Glassy carbon substrates were first polished with polishing alumina, followed by flushing with water and ethanol, and then were sonicated in ethanol before use. The cleaned glassy carbon substrates were then used for deposition of PTTB by CV. When an FTO or a glassy carbon sheet was used as working electrode, the surface was controlled to expose $1 \times 1 \text{ cm}^2$ by covering tape. The polymer-grafted electrodes were rinsed thoroughly with dichloromethane or acetonitrile and dried under air; afterward dipped in 1 mM Cosalen methanol solution for 10 h to assemble the molecular catalyst, which were then rinsed with methanol thoroughly and dried under air. FTO used as substrate to grow PTTB was first sonicated in isopropanol, water, and ethanol in sequence for cleanliness, followed by polymer deposition and catalyst assembly as performed on glassy carbon substrates.

Electrochemical Methods for Hydrogen Evolution: Electrochemistry experiments were conducted using a CHI 600E. The LSV and CV measurements were conducted in a three-electrode configuration electrochemical cell (1 chamber) under an inert nitrogen atmosphere using the fabricated glassy carbon rods as the working electrode, a platinum wire as the auxiliary (counter) electrode, and an $\text{Ag}/\text{AgCl}/3 \text{ M KCl}$ electrode as the reference electrode. The Ag/AgCl electrode was calibrated with a reversible hydrogen electrode (see Figure S14, Supporting Information). The potentials in electrocatalytic hydrogen evolution studies were converted to RHE by adding a value of $(0.186 + 0.059 \text{ pH}) \text{ V}$.

CPE measurements to determine Faradaic efficiency and study long-term stability were conducted in a sealed two-chambered H cell where the first chamber held the glassy carbon sheet working electrode and Ag/AgCl reference electrode in 50 mL of 0.1 M HAc/NaAc buffer (aq) at the corresponding pH, and the second chamber held the auxiliary electrode in 50 mL of 0.1 M HAc/NaAc buffer (aq) at the corresponding pH. The two chambers, which were both under a N_2 atmosphere, were separated by a proton exchange membrane. Continuous stirring was conducted during the electrolysis to get rid of the bubble adhering on the surface of the fabricated electrode. The amount of hydrogen produced was quantified by gas chromatography. The faradaic efficiencies were calculated using the following equation:

$$\text{Faradic yield} = 100 \times \frac{2F[\text{H}_2]}{Q} \quad (1)$$

where F is the Faraday constant (C mol^{-1}), $[\text{H}_2]$ (mol) is the amount of hydrogen measured in the headspace, and Q (C) is the charged passed during electrolysis.

$$\text{TON} = \frac{\text{number of H}_2 \text{ molecules}}{\text{number of catalyst molecules}} \quad (2)$$

$$\text{TOF} = \frac{\text{TON}}{\text{electrolysis time}} \quad (3)$$

Physical Methods: FTIR spectra were acquired using a Bruker INVENIO R spectrometer. Samples for analysis were mixed into a KBr matrix and pressed into pellets. The samples for FTIR were collected by peeling off the films on the hard electrodes. UV–vis absorption spectra were measured with a Cary 60 UV–vis spectrophotometer.

To measure the catalyst loading, ICP-MS was performed using an Agilent 7900 ICP-MS. A 0–100 ppb cobalt standard in nitric acid (Sigma-Aldrich) was used to construct a calibration plot. The ICP-MS samples were prepared by immersing a GC/PTTB/Cosalen wafer into 5 mL aqua regia solution, followed by sonicating the solution for 1 h. The solution was then diluted to 50 mL with deionized water. The Co concentration in the solution was analyzed by ICP-MS and was converted to the Cosalen with the same quantities. The maximum Cosalen concentration on the electrode was then calculated from the acquired Cosalen amount divided by the exposed area of the electrode. Following CPE experiments, the pH 4.5 solutions were collected, filtered, and analyzed by ICP-MS to determine if any cobalt material was solubilized during the experiment. Relative solvents were analyzed as controls. The trace amounts of cobalt in these controls were averaged and subtracted from the cobalt concentrations.

XPS data were collected using a PHI5000 VersaProbeIII XPS instrument (ULVAC-PHI). The monochromatic X-ray source was the Al K α line at 1486.6 eV, directed at 45° to the sample surface. Low-resolution survey spectra were acquired between binding energies of 0–1100 eV. Higher-resolution detailed scans, with a resolution of ≈ 0.1 eV, were collected on individual XPS lines of interest. The XPS data were analyzed using a Multipak software. The samples for XPS were prepared by peeling off the films on the hard electrodes.

The surface morphology of the substrates was characterized using a field emission scanning electron microscope (Hitachi SU8010, Japan). Samples on SEM electrode were used to watch the morphology. Cross-sectional SEM was performed with samples on glassy carbon sheet and was obtained after depositing a protective layer of Pt. TEM was conducted on a Talos F200X microscope (USA). Samples for TEM were first fabricated on FTO, and then collected in ethanol, followed with sonicating for 10 min.

The amount of gaseous H₂ was detected and quantified by headspace gas analysis after electrolysis using an Agilent 7890A Series gas chromatography equipped with a 5 Å molecular sieve column (Ar carrier gas at a flow rate of approximately 3 mL min⁻¹).

Supporting Information

Supporting Information is available from the Wiley Online Library or from the author.

Acknowledgements

This work was supported by Research Plan-Science & Technology Department of Shaanxi Province (grant no. 2017JQ2012), Natural Science Research Program Education Department of Shaanxi Province (grant no. 15JK1708), and Shaanxi Key Research grant (China, 2020GY-244). J.T. thanks EPSRC (EP/S018204/2) and Royal Society-Newton Advanced Fellowship grants (NA170422 and NAF\191163).

Conflict of Interest

The authors declare no conflict of interest.

Keywords

cobalt, electrochemical hydrogen evolution, molecular catalysts, polymers

Received: June 5, 2020

Revised: July 22, 2020

Published online:

- [1] N. Plumeré, O. Rüdiger, A. A. Oughli, R. Williams, J. Vivekananthan, S. Pöller, W. Schuhmann, W. Lubitz, *Nat. Chem.* **2014**, *6*, 822.
- [2] a) D. Khusnutdinova, A. M. Beiler, B. L. Wadsworth, S. I. Jacob, G. F. Moore, *Chem. Sci.* **2017**, *8*, 253; b) L. Yuan, C. Han, M.-Q. Yang, Y.-J. Xu, *Int. Rev. Phys. Chem.* **2016**, *35*, 1.
- [3] K. E. Dalle, J. Warnan, J. J. Leung, B. Reuillard, I. S. Karmel, E. Reisner, *Chem. Rev.* **2019**, *119*, 2752.
- [4] a) C. E. Creissen, J. Warnan, E. Reisner, *Chem. Sci.* **2018**, *9*, 1439; b) M. Wang, Y. Yang, J. Shen, J. Jiang, L. Sun, *Sustainable Energy Fuels* **2017**, *1*, 1641; c) N. Kaeffer, J. Massin, C. Lebrun, O. Renault, M. Chavarot-Kerlidou, V. Artero, *J. Am. Chem. Soc.* **2016**, *138*, 12308.
- [5] a) E. S. Andreiadis, P.-A. Jacques, P. D. Tran, A. Leyris, M. Chavarot-Kerlidou, B. Joussetme, M. Matheron, J. Pécaut, S. Palacin, M. Fontecave, V. Artero, *Nat. Chem.* **2013**, *5*, 48; b) N. Kaeffer, A. Morozan, V. Artero, *J. Phys. Chem. B* **2015**, *119*, 13707; c) P. D. Tran, A. LeGoff, J. Heidkamp, B. Joussetme, N. Guillet, S. Palacin, H. Dau, M. Fontecave, V. Artero, *Angew. Chem.* **2011**, *123*, 1407; d) B. Reuillard, J. Warnan, J. J. Leung, D. W. Wakerley, E. Reisner, *Angew. Chem. Int. Ed.* **2016**, *55*, 3952; e) Y. Chen, H. Chen, H. Tian, *Chem. Commun.* **2015**, *51*, 11508; f) A. Le Goff, V. Artero, B. Joussetme, P. D. Tran, N. Guillet, R. Métayé, A. Fihri, S. Palacin, M. Fontecave, *Science* **2009**, *326*, 1384; g) S. C. Eady, M. M. MacInnes, N. Lehnert, *Inorg. Chem.* **2017**, *56*, 11654.
- [6] a) B. L. Wadsworth, D. Khusnutdinova, G. F. Moore, *J. Mater. Chem. A* **2018**, *6*, 21654; b) R. M. Kellett, T. G. Spiro, *Inorg. Chem.* **1985**, *24*, 2378; c) A. J. Clough, J. W. Yoo, M. H. Mecklenburg, S. C. Marinescu, *J. Am. Chem. Soc.* **2015**, *137*, 118; d) C. A. Downes, S. C. Marinescu, *Dalton Trans.* **2016**, *45*, 19311; e) C. A. Downes, S. C. Marinescu, *J. Am. Chem. Soc.* **2015**, *137*, 13740; f) B. L. Wadsworth, A. M. Beiler, D. Khusnutdinova, S. I. Jacob, G. F. Moore, *ACS Catal.* **2016**, *6*, 8048.
- [7] S. C. Eady, S. L. Peczonczyk, S. Maldonado, N. Lehnert, *Chem. Commun.* **2014**, *50*, 8065.
- [8] A. M. Beiler, D. Khusnutdinova, S. I. Jacob, G. F. Moore, *ACS Appl. Mater. Interfaces* **2016**, *8*, 10038.
- [9] a) Q. Zhou, G. Shi, *J. Am. Chem. Soc.* **2016**, *138*, 2868; b) S. Bai, Q. Hu, Q. Zeng, M. Wang, L. Wang, *ACS Appl. Mater. Interfaces* **2018**, *10*, 11319; c) P. Chmielarz, M. Fantin, S. Park, A. A. Isse, A. Gennaro, A. J. D. Magenau, A. Sobkowiak, K. Matyjaszewski, *Prog. Polym. Sci.* **2017**, *69*, 47.
- [10] a) C.-B. Li, Y. Chu, J. He, J. Xie, J. Liu, N. Wang, J. Tang, *ChemCatChem* **2019**, *11*, 6324; b) C.-B. Li, P. Gong, Y. Yang, H.-Y. Wang, *Catal. Lett.* **2018**, *148*, 3158; c) R. M. Irfan, D. Jiang, Z. Sun, L. Zhang, S. Cui, P. Du, *J. Catal.* **2017**, *353*, 274; d) H. Chen, Z. Sun, S. Ye, D. Lu, P. Du, *J. Mater. Chem. A* **2015**, *3*, 15729.
- [11] a) P. G. Cozzi, *Chem. Soc. Rev.* **2004**, *33*, 410; b) R. M. Clarke, T. Storr, *Dalton Trans.* **2014**, *43*, 9380.
- [12] T. J. Chuang, C. R. Brundle, D. W. Rice, *Surf. Sci.* **1976**, *59*, 413.
- [13] D. Schilter, J. M. Camara, M. T. Huynh, S. Hammes-Schiffer, T. B. Rauchfuss, *Chem. Rev.* **2016**, *116*, 8693.
- [14] N. Kaeffer, M. Chavarot-Kerlidou, V. Artero, *Acc. Chem. Res.* **2015**, *48*, 1286.
- [15] S. Hiroto, Y. Miyake, H. Shinokubo, *Chem. Rev.* **2016**, *117*, 2910.

- [16] S. Rioual, B. Lescop, F. Quentel, F. Gloaguen, *Phys. Chem. Chem. Phys.* **2015**, *17*, 13374.
- [17] Y. Zhang, Y. Liu, M. Ma, X. Ren, Z. Liu, G. Du, A. M. Asiri, X. Sun, *Chem. Commun.* **2017**, *53*, 11048.
- [18] F. Zhao, J. Zhang, T. Abe, D. Wöhrle, M. Kaneko, *J. Mol. Catal. A: Chem.* **1999**, *145*, 245.
- [19] a) S. Cobo, J. Heidkamp, P.-A. Jacques, J. Fize, V. Fourmond, L. Guetaz, B. Joussetme, V. Ivanova, H. Dau, S. Palacin, M. Fontecave, V. Artero, *Nat Mater* **2012**, *11*, 802; b) J. A. Widegren, R. G. Finke, *J. Mol. Catal. A: Chem.* **2003**, *198*, 317; c) E. Anxolabéhère-Mallart, C. Costentin, M. Fournier, S. Nowak, M. Robert, J.-M. Savéant, *J. Am. Chem. Soc.* **2012**, *134*, 6104.